

# Accretion during binary star formation – II. Gaseous accretion and disc formation

Matthew R. Bate<sup>1,2</sup> and Ian A. Bonnell<sup>1</sup>

<sup>1</sup>*Institute of Astronomy, Madingley Road, Cambridge CB3 0HA*

<sup>2</sup>*Max-Planck-Institut für Astronomie, Königstuhl 17, D-69117 Heidelberg, Germany*

Accepted 1996 September 10. Received 1996 August 28; in original form 1996 May 2

## ABSTRACT

We consider the effects of accretion during binary star formation. When a ‘seed’ protobinary system forms within a collapsing molecular cloud core, its final state is determined by the accretion of, or interaction with, the remaining cloud material as it falls on to the system. The mass ratio and orbit of the binary and the formation of circumstellar and circumbinary discs are all dependent on the dynamics of this accretion process.

In this paper, we study the effects of accretion on the mass ratio and separation of the binary. The gas is modelled using smoothed particle hydrodynamics (SPH), and the results are compared and contrasted with those obtained using ballistic calculations in an earlier paper. The inclusion of hydrodynamic effects also allows us to study the disc formation process. We determine what fractions of the infalling gas form circumstellar and circumbinary discs and find that, under some circumstances, a large circumstellar disc forms around the primary while the secondary has only a small circumstellar disc, or indeed no disc at all. The observational implications are discussed.

**Key words:** accretion, accretion discs – hydrodynamics – binaries: general – circumstellar matter – stars: formation.

## 1 INTRODUCTION

Recent observations of main-sequence stellar systems show that most stars are members of binary or multiple systems (Duquennoy & Mayor 1991; Fischer & Marcy 1992; Mayor et al. 1992). Furthermore, pre-main-sequence surveys (Mathieu, Walter & Myers 1989; Simon et al. 1992; Ghez, Neugebauer & Matthews 1993; Leinert et al. 1993; Reipurth & Zinnecker 1993) give an excess of companions over the main sequence in most of the separation ranges surveyed, demonstrating that star formation must predominantly produce multiple systems.

The main-sequence G-dwarf survey of Duquennoy & Mayor (1991) provides various statistical properties of binary systems. Binaries are found to have separations ranging from a few  $R_{\odot}$  to  $10^4$  au, and their mass-ratio distribution increases towards small mass ratios. There is also weak evidence that the overall mass-ratio distribution differs from that for short-period systems. The distribution for close binaries is consistent with a uniform distribution, or

possibly rising towards mass ratios of unity (Mazeh et al. 1992). This result is yet to be confirmed.

For pre-main-sequence binary systems the mass and orbital statistics are less well known. However, thus far, they appear to be similar to those observed for the main-sequence systems of Duquennoy & Mayor (1991) (Mathieu 1992a,b; Leinert et al. 1993; Reipurth & Zinnecker 1993). Hence these properties must be determined early in the star formation process. In addition, pre-main-sequence systems often show evidence for circumstellar and circumbinary material left over from the star formation process. At least 50 per cent of pre-main-sequence binaries have excess flux associated with circumstellar and/or circumbinary discs (Strom et al. 1989; Strutskie et al. 1990). Recently, a circumbinary disc has been directly imaged around GG Tau (Dutrey, Guilloteau & Simon 1994). Finally, a surprising finding has been the discovery of infrared companions, where an optically visible pre-main-sequence star has a deeply embedded companion visible only in the infrared (Mathieu 1994, and references within), even though the two

stars are supposedly coeval. Zinnecker & Wilking (1992) estimate the frequency of infrared companions to be  $\sim 10$  per cent of all T Tauri binary systems. It is also common for the infrared companions to be more luminous than their optical counterparts (e.g. Chelli et al. 1988). Typical separations of these objects are  $\sim 100$  au.

The favoured mechanism for producing this wide range of binary systems is the fragmentation of a molecular cloud core during its gravitational collapse. Fragmentation can be divided into two main classes: thermal fragmentation (e.g. Boss & Bodenheimer 1979; Boss 1986; Bonnell et al. 1991, 1992; Bonnell & Bastien 1992; Nelson & Papaloizou 1993), and disc fragmentation (Adams, Ruden & Shu 1989; Shu et al. 1990; Heemskerk, Papaloizou & Savonije 1992; Bonnell 1994; Bonnell & Bate 1994a,b; Woodward, Tohline & Hachisu 1994). In both cases, the binary or multiple protostellar systems that are initially formed contain only a small fraction of the total mass of the original cloud. The size of this fraction decreases with the initial separation of the binary (Boss 1986; Bonnell & Bate 1994b). Thus the final state of the binary depends on the accretion of, and interaction with, the remaining cloud material as it falls on the system. As the system grows in mass, its mass ratio, separation and eccentricity change. The infalling material is also responsible for the formation of circumstellar and circum-binary discs.

In this study, we do not attempt to follow the evolution of such ‘seed’ binary systems as they accrete their remaining gas clouds. The number of possible cloud configurations and initial binary parameters, and the resolution required to accurately follow such calculations prohibits this. Rather, we assume that a ‘seed’ binary is formed via a fragmentation process and seek to determine, given the accretion of a small amount of gas with known characteristics, how the system changes. This approach allows for the evaluation of the effects of accretion for arbitrary cloud configurations and initial ‘seed’ binaries.

We investigate the effects of accretion on the mass ratio and separation of a protobinary as functions of the initial mass ratio of the binary and the specific angular momentum of the infalling cloud material. These effects were investigated in a previous paper (Bate 1997, hereafter Paper I) by modelling the ‘gas’ cloud with ballistic particles, without hydrodynamic forces. The protobinary was modelled by two point masses, each of which had an accretion radius defined so that whenever a ‘gas’ particle passed within this radius its mass and momentum were added to the protostar, and the particle was removed. To investigate the dependence of the results on the accretion radii, calculations were performed with accretion radii of  $1/20$  of the separation of the binary, and with accretion radii equal to the mean Roche lobe sizes (Frank, King & Raine 1985) of the protostars. It was found that, qualitatively, the mass ratio and separation decrease for the accretion of matter with low specific angular momentum, and increase for the accretion of matter with high specific angular momentum material. Quantitatively, however, the results depended critically on the assumed accretion radii of the protostars, and, especially for infall with high specific angular momentum, on the initial radial-infall velocity the particles had when they were injected into the simulations at the outer boundary of the cloud.

In this paper, we study the effects of gaseous accretion on a protobinary system. Instead of modelling the gas cloud with ballistic particles, pressure and viscous forces are included by modelling the gas using smoothed particle hydrodynamics (SPH). The inclusion of hydrodynamics removes the dependence of the results on the assumed sizes of the protostars, as circumstellar discs are free to form around the protostars via dissipation. Circumstellar disc formation is studied directly, and the formation of circum-binary discs is investigated which was impossible with the dissipativeless calculations of Paper I. Only initially circular ‘seed’ binaries are considered and the gas is non-self-gravitating, with a mass very much less than that of the binary.

In Section 2, we describe the SPH code and the method for modelling the protostars. Details of the numerical calculations are given in Section 3. The dynamics of the accretion, including a study of disc formation, are presented in Section 4. The effects of accretion on the mass ratio and separation of the protobinary are given in Sections 5 and 6, respectively. We discuss how these results depend on the radial-infall velocity of the gas in Section 7. In Section 8, the results are compared and contrasted with those obtained in Paper I using ballistic accretion. Finally, the observational implications are given in Section 9, and the conclusions are given in Section 10.

## 2 COMPUTATIONAL METHOD

The calculations presented here were performed using a three-dimensional SPH code based on a version originally developed by Benz (Benz 1990; Benz et al. 1990). The code uses a tree to find the nearest neighbours. The standard form of artificial viscosity is used (Monaghan & Gingold 1983; Benz 1990; Monaghan 1992), with the parameters  $\alpha = 1$  and  $\beta = 2$ . The SPH equations are integrated using a second-order Runge–Kutta–Fehlberg integrator.

Several alterations have been made to the original SPH code, the most important of which are the addition of individual time-steps for each particle and the inclusion of sink particles. These are described fully by Bate (1995) and Bate, Bonnell & Price (1995). Only a brief description of sink particles will be given here.

Sink particles were developed to allow calculations with large density contrasts (e.g. fragmentation calculations) to be followed in a realistic amount of computational time. In SPH, a high-density region of gas is represented by many gas particles in a small volume. Small time-steps are required to evolve these particles correctly. If the particles form a bound object, they can be replaced by a single ‘sink’ particle which has their combined mass and momentum. This sink particle accretes any SPH particles if they fall within a certain radius, the accretion radius,  $r_{\text{acc}}$ , of the sink particle, and if they are bound to the sink particle. In this way, the high-density gas within bound fragments is ignored, and it does not contribute to the computations.

Sink particles interact with SPH gas particles only via gravitational forces and through boundary conditions for particles near the accretion radius (Bate et al. 1995). Boundary conditions are required in some situations so that the presence of a sink particle and its evacuated accretion radius do not adversely affect the gas outside  $r_{\text{acc}}$ . They are not required if the radial-infall velocity of the gas at the

accretion radius is supersonic and large compared to the rotational velocity of the gas (e.g., supersonic, spherical accretion). They are also not required if the flow of gas past a sink particle is supersonic and fast compared to the SPH viscous time-scale (e.g. Bondi–Hoyle accretion). If these conditions apply, pressure and viscous discontinuities at the accretion radius cannot propagate outwards (Bate 1995; Bate et al. 1995). Boundary conditions are often required for simulations in which discs are formed around sink particles. Otherwise, the shear viscosity present in SPH, and its discontinuity at the accretion radius, quickly erodes the disc from the inside out (Bate et al. 1995). This is not a problem if the disc is continually being replenished by accretion, since only the inner parts of the disc will be affected and the outer parts will still be resolved. If the disc is not replenished fast enough, however, the outer parts of the disc are not resolved and the flow of gas near the disc is incorrectly modelled.

In the calculations presented here, sink particles are used to model the protostars of the ‘seed’ binary. The infalling gas is non-self-gravitating, and thus the only gravitational forces present are those from the sink particles. Sink particle boundary conditions are not used in calculations where accretion on to one or both of the protostars proceeds via a Bondi–Hoyle-type accretion stream. This is possible in the cases where a circumstellar disc is formed around one of the protostars, because the accretion rate on to the disc is always very high and hence the disc remains resolved. For calculations where two circumstellar discs are formed and the accretion rates on to these discs are low, however, boundary conditions are required to resolve the discs.

### 3 NUMERICAL CALCULATIONS

The method used to study gaseous accretion is similar to that used in Paper I for ballistic accretion. This allows direct comparison between the ballistic and gaseous results.

#### 3.1 Modelling the protostars

The binary protostellar system is modelled by sink particles, as described above. The masses of the primary and secondary are  $M_1$  and  $M_2$ , respectively. The binary has mass ratio  $q = M_2/M_1$ , total mass  $M_b$ , and separation  $a$ . Only binaries with initially circular orbits are considered. Natural units are used with the gravitational constant  $G = 1$  and, initially,  $M_b = 1$  and  $a = D = 1$ . For this choice of units, a particle that is in a circular orbit around a mass  $M_b$  at a radius  $r = D$  has a specific angular momentum  $j$  of unity (i.e.,  $j_{\text{circ}} = \sqrt{GM_b D} = 1$ ). Also, note that since  $M_b = 1$  and  $a = 1$  initially, then  $\dot{M}_b$  and  $\dot{a}$  are the fractional changes in  $M_b$  and  $a$  with time. Thus, for example,  $\dot{q}/M_b = \dot{q}/(M_b/M_b)$  and  $\dot{a}/M_b = (\dot{a}/a)/(M_b/M_b)$ .

The sink particles have accretion radii of  $r_{\text{acc}} = 0.05D$ . To ensure that the results do not depend on the accretion radii, some calculations were also performed with  $r_{\text{acc}} = 0.02D$ . The results were the same for both values of the accretion radii within the estimated errors.

#### 3.2 Modelling the gas cloud

The protobinary is embedded in a gas cloud that is modelled by SPH particles. This gas falls on to the binary system and

is accreted by, or otherwise interacts with, the binary. To maintain the cloud during the simulation, particles are injected at the outer boundary of the simulation at a radius  $R = 8D$  from the centre of mass of the binary. The axis of rotation of the cloud is the same as the axis of rotation of the binary, and the cloud is either stationary or is rotating in the same sense as the binary. These assumptions are justified, as it is envisaged that the infalling gas is from the cloud out of which the protobinary formed.

As in Paper I, we specify that a given simulation has *each* particle injected with the *same* specific angular momentum. This allows us to study the effects of accretion as functions of the mass ratio of the binary  $q$ , and the specific angular momentum of the infalling gas  $j_{\text{inf}}$ . Thus the initial tangential velocity of a particle around the centre of mass is  $v_t = j_{\text{inf}}/r_{\text{xy}}$ , where  $r_{\text{xy}}$  is the cylindrical radius from the axis of rotation of the binary. In addition to the tangential velocity, the radial-infall velocity of the particles at the outer boundary of the calculation can be varied. This is set as some fraction  $v_{\text{rad}}$  of the radial velocity a particle would have after a free-fall from infinity

$$v_r = v_{\text{rad}} \sqrt{\frac{2GM_b}{r} - \frac{j_{\text{inf}}^2}{r_{\text{xy}}^2}}, \quad (1)$$

where, for  $v_{\text{rad}} = 1$ , the kinetic energy of the particle is equal to the gravitational energy liberated during its fall. The effect of varying  $v_{\text{rad}}$  is studied in Section 7 by performing some calculations with both  $v_{\text{rad}} = 0$  and  $v_{\text{rad}} = 1$ .

Due to the rotation of the cloud, each particle has a centrifugal acceleration acting upon it. Clearly, a particle should not be injected at any position for which the centrifugal acceleration is not balanced or exceeded by the acceleration due to gravity from the binary. Thus particles are injected into the simulation randomly over the surface of the sphere of radius  $R$ , with uniform surface density modified by the criterion that

$$\frac{v_t^2}{r_{\text{xy}}} \leq \frac{GM_b}{R^2} \frac{r_{\text{xy}}}{R}. \quad (2)$$

For a stationary cloud, particles are injected at any position on the spherical surface of radius  $R$  with equal likelihood. For rotating clouds, no particles are injected near the poles of the sphere. Hence there is a cone-shaped hole in the gas cloud above and below the orbital plane of the binary.

A fixed number of particles per unit time are injected at the outer boundary of the cloud. The injection rate is determined by ensuring there are a constant number of particles  $N$  between  $r = R$  and  $r = R - D$ . When a particle falls out of this shell, a new particle is injected at  $r = R$ . In the calculations presented here,  $N = 800$  with  $v_{\text{rad}} = 1$ , and  $N = 3000$  with  $v_{\text{rad}} = 0$ . Calculations with a  $q = 0.6$  binary, over the full range of values of  $j_{\text{inf}}$ , were also performed with  $N = 3000$  and  $v_{\text{rad}} = 1$  to ensure that the resolution of the calculations does not affect the results. The results were the same for both particle injection rates, within the estimated errors. The mass of each gas particle is  $m = 5 \times 10^{-7} M_b$ , and the calculations are typically evolved until  $\approx 2 \times 10^4$  particles have been injected.

Finally, we use an isothermal equation of state

$$P = c_s^2 \rho, \quad (3)$$

where  $P$  is the pressure,  $\rho$  is the density, and  $c_s$  is the sound speed of the gas. The temperature is chosen so as to make the gas ‘cold’ (i.e. pressure forces are not dynamically important). Pressure forces at the outer boundary of the calculations are of order 1/10 of the gravitational forces from the binary. The ratio of the sound speed of the gas to the orbital velocity at  $r = D$  is  $c_s/v_D = 0.056$ . For this ratio, the temperature of the gas is 10 K for a binary of mass  $M_b = 1 M_\odot$  and separation  $D = 10^{15}$  cm. To confirm that the results are indeed representative of a ‘cold’ gas, additional calculations were performed with  $q = 0.2$  and  $q = 0.6$  binaries where the temperature of the gas was reduced by an order of magnitude (i.e.  $c_s/v_D = 0.018$ ). The results from these calculations were identical (within the estimated errors) to those obtained with the higher temperature. Thus the gas is dynamically cold. We do not study how the results are altered if pressure is dynamically important.

### 3.3 Analysis of the results

We define the mass of a protostar ( $M_1$  or  $M_2$ ) to be the mass of a sink particle and its circumstellar disc (if any). This definition is used because, in the majority of cases, most of the material captured by a protostar is contained in its circumstellar disc and only a small fraction is actually accreted by the sink particle during a calculation. Thus the binary mass  $M_b$  is equal to the masses of the sink particles and their circumstellar discs. The binary’s orbit is calculated by considering these masses. A gas particle belongs to a circumstellar disc if its orbit, calculated considering only one protostar at a time, has eccentricity  $e < 0.5$ , and semi-major axis  $a < D/2$ . This simple criterion gives excellent circumstellar-disc extraction.

The gas injected into the simulation,  $M_{\text{inf}}$ , and the amount of gas that is not captured by one of the protostars (circumbinary mass),  $M_{\text{cb}} = M_{\text{inf}} - M_1 - M_2$ , are also determined. If there is no circumbinary disc, the circumbinary mass remains constant after steady accretion has been attained, whereas if a circumbinary disc forms,  $M_{\text{cb}}$  increases uniformly with time. The total angular momentum of the circumbinary material  $L_{\text{cb}} = j_{\text{cb}} M_{\text{cb}}$  is monitored. Without a circumbinary disc,  $j_{\text{cb}} = j_{\text{inf}}$ . However, if a circumbinary disc forms, the binary can lose orbital angular momentum to the circumbinary disc via gravitational torques (see Sections 4 and 6), and  $j_{\text{cb}}$  increases.

The calculations are run until the accretion rates on to the circumstellar discs and/or sink particles have become steady, at which point the effects of accretion on the binary are calculated over a few orbits. Thus the effects that are determined assume that the accretion flow is in approximate steady-state over an orbital time-scale. The accretion rates  $\dot{M}_1$  and  $\dot{M}_2$ , the rate of change of semimajor axis  $\dot{a}$ , the gas infall rate  $\dot{M}_{\text{inf}}$ , the rate of increase of the circumbinary material  $\dot{M}_{\text{cb}}$ , and its total angular momentum  $\dot{L}_{\text{cb}}$  are determined by linear regressions as functions of time. The linear regressions are performed only over the period where the accretion rates are constant. Error estimates for each quantity are obtained from the linear regression. For the accre-

tion rates, these errors are combined with  $\sqrt{N}/N$  statistical errors, where  $N$  is the number of particles accreted over the time period of the regressions. Generally, these errors provide a good estimate of the true errors in the quantities. The rate of change of mass ratio is given by

$$\dot{q} = (\dot{M}_2 - q\dot{M}_1) \frac{(1+q)}{M_b}. \quad (4)$$

The effects of accretion on orbital eccentricity are not studied, as the binaries are all in circular orbits initially. As was observed in Paper I, however, a small eccentricity grows at the beginning of each simulation, since eccentricity is always positive and, thus, any force on the binary produces a non-zero eccentricity. The evolution of this eccentricity is for it to grow initially, and then to oscillate in a sinusoidal pattern with approximately constant amplitude. For all simulations the eccentricity remains small ( $e \lesssim 0.002$ ) throughout. Eccentricity is expected to grow when a binary is surrounded by a circumbinary disc (Artymowicz et al. 1991), but this is not detected here because the disc has such a low mass compared to the binary and the system is only evolved over a few orbits ( $\lesssim 5$ ). The period of the oscillation is equal to the orbital period of the binary. Such periodic changes of orbital elements are known from analytic solutions of binary motion under a perturbing force (Kopal 1959). As with ballistic accretion, the oscillations display no noticeable dependence on the mass ratio of the binary, but the amplitude decreases with increasing angular momentum of the cloud.

## 4 ACCRETION DYNAMICS

The infall of gas on to a protobinary system allows the formation of circumstellar and circumbinary discs. We now consider the dynamics of this accretion for binaries with mass ratios  $0.1 \leq q \leq 1.0$  under the infall of gas with specific angular momentum in the range  $0 \leq j_{\text{inf}} \leq 2$ . In all cases  $v_{\text{rad}} = 1$ .

### 4.1 Accretion dynamics and disc formation

Figs 1 and 2 show the distributions of gas around binaries with mass ratios of  $q = 0.2$  and  $q = 0.6$ , respectively, once steady accretion on to the components and/or the circumstellar discs of the binaries has been attained. The gas distributions are given as a function of the specific angular momentum of the infalling gas  $j_{\text{inf}}$ .

A general progression is observed with increasing  $j_{\text{inf}}$  (e.g. Fig. 2). With most mass ratios, under infall with zero angular momentum, no discs are formed outside the accretion radii of the sink particles ( $r_{\text{acc}} = 0.05D$ ). When the angular momentum of the cloud is increased, a circumprimary disc is formed. For still higher angular momenta, both circumprimary and circumsecondary discs are formed. The value of  $j_{\text{inf}}$  above which a circumsecondary disc forms depends on the binary’s mass ratio (cf. Figs 1 and 2). With angular momenta of  $j_{\text{inf}} \approx 1$ , two circumstellar discs are formed, and the formation of a circumbinary disc begins. Spiral density waves are produced in the circumbinary material via gravitational torques from the binary. At still higher  $j_{\text{inf}}$ , a region of exclusion appears near the binary where little or no gas is

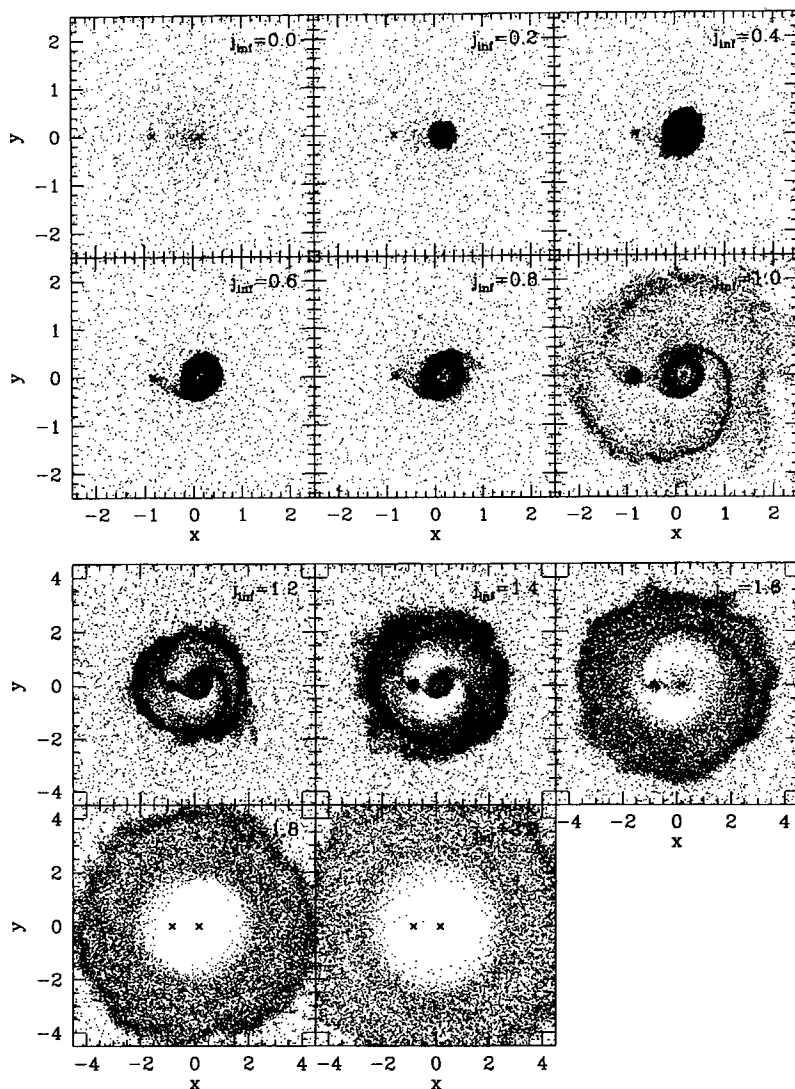


**Figure 1.** Steady-state accretion on to a  $q=0.2$  protobinary system from clouds with various specific angular momenta  $j_{\text{inf}}$ . The protostars are marked with crosses, with the primary on the right. Gas particle positions are projected on to the plane of the binary. Axes are given in units of the binary's separation  $D$ . Rotation is anticlockwise.

present. The infalling gas has too much angular momentum to occupy this region. However, accretion does proceed on to the circumstellar discs from the circumbinary disc via streams of gas which lose angular momentum due to gravitational torques from the binary. The amount of material accreted by the circumstellar discs decreases with increasing  $j_{\text{inf}}$ , with the result that the circumstellar discs are unresolved for  $j_{\text{inf}} \gtrsim 1.4$ . Finally, for the material with highest angular momentum, all the gas goes into a circumbinary disc. The binary is unable to perturb this disc strongly enough for gas to be accreted on to the circumstellar discs.

Velocity plots and density contours of the accretion flows are shown for a  $q=0.6$  protobinary in Fig. 3. For  $j_{\text{inf}}=0$  (Fig. 3a), a small disc is formed around the primary, just outside the accretion radius of the sink particle ( $r_{\text{acc}}=0.05D$ ). Accretion on to this disc occurs mainly from a stream impacting the disc on its inside-trailing edge. For the secondary, no disc is resolved. Instead, the material cap-

tured by the secondary forms a Bondi–Hoyle-type accretion stream. Infalling material passes around both the leading and trailing sides of the secondary, is gravitationally focused, collides inside the orbit of the secondary, and dissipates most of its kinetic energy. Material that is bound to the secondary (i.e. roughly inside its Roche lobe) then falls back towards the secondary to be accreted by it in a Bondi–Hoyle-type flow. This material is accreted on the inside-trailing edge of the sink particle.

For  $j_{\text{inf}}=0.4$  (Fig. 3b), the flow pattern is similar. The specific angular momentum of the material forming the circumprimary disc is larger than with  $j_{\text{inf}}=0$ , and hence the disc extends to a larger radius from the primary. Again, accretion on to this disc occurs on its inside-trailing edge. The secondary does not form a resolved disc, as the gas still does not have sufficient angular momentum, and accretion proceeds via a Bondi–Hoyle-type stream as with  $j_{\text{inf}}=0$ .

Discs form around both protostars for  $j_{\text{inf}}=0.8$  (Fig. 3c).

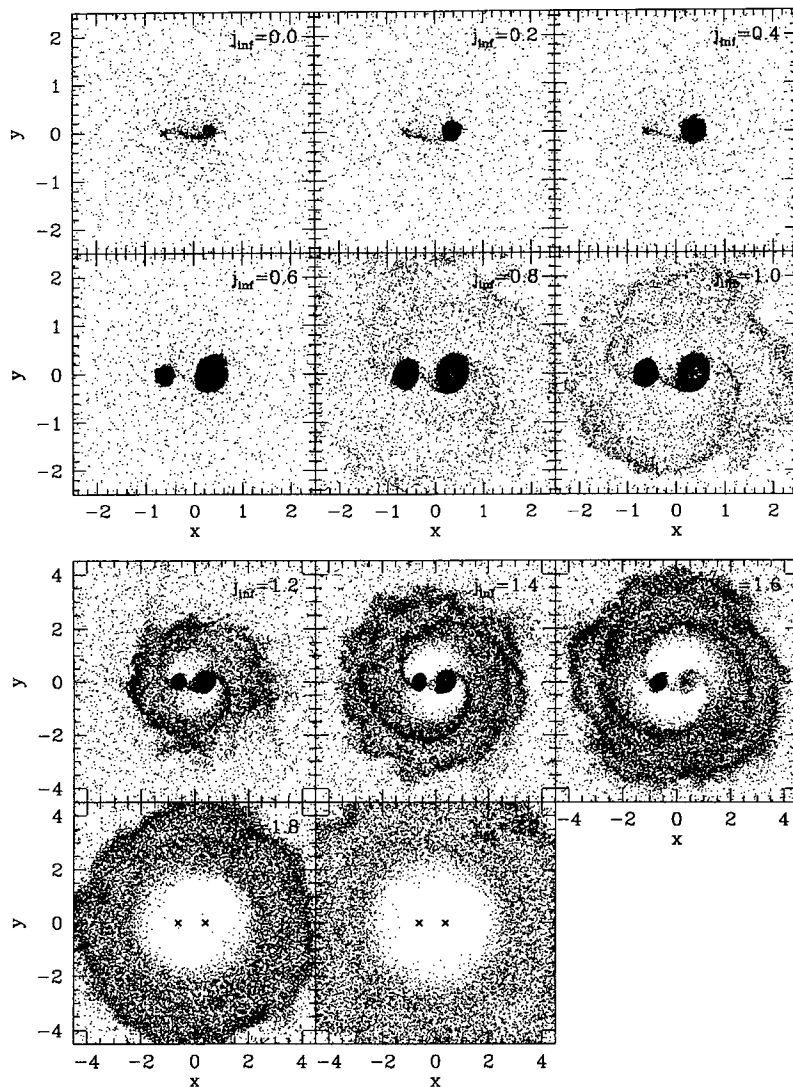


**Figure 2.** Steady-state accretion on to a  $q=0.6$  protobinary system from clouds with various specific angular momenta  $j_{\text{inf}}$ . The protostars are marked with crosses, with the primary on the right. Gas particle positions are projected on to the plane of the binary. Axes are given in units of the binary's separation  $D$ . Rotation is anticlockwise.

The infalling material now has enough angular momentum to form a disc around the secondary (see Section 4.2). The gas has too much angular momentum to fall in behind the secondary, so that no material collides with that which is captured from the leading side of the secondary. Hence a disc is formed, rather than a Bondi–Hoyle-type accretion stream. The increased angular momentum also results in the dominant accretion on to the circumprimary disc coming from its leading-outside edge. Finally, there is a build-up of circumbinary material. Some of the infalling gas extracts enough angular momentum from the binary to avoid accretion on to the circumstellar discs. Spiral density waves are produced in this material due to the torques from the binary.

With  $j_{\text{inf}}=1.4$  (Fig. 3d), the infalling gas has too much angular momentum to fall directly on to the binary, and a distinct circumbinary disc is formed with a void, essentially free of gas, inside. The radius of the inner edge of the disc

is roughly equal to the periastron distance to which the gas would fall in if the binary were replaced by a single point mass. Accretion on to the binary proceeds via tidal distortion of the inner edge of the disc. Material in the disc ahead of one of the components is slowed by the gravity of the protostar and falls into a lower orbit because of the loss of angular momentum. As the protostar approaches, this loss of angular momentum increases and it continues to fall in. If it falls within the outer Lagrange point, it is captured by the protostar and forms a circumstellar disc. Material that does not pass within the outer Lagrange point is accelerated by the gravity of the protostar once it is overtaken by the protostar, gaining angular momentum and moving outward again. This produces the spiral density waves that penetrate out into the disc as the gas collides with the slower material in front of it. The material accreted by the circumstellar discs has very high angular momentum – just low enough for it to pass within the outer Lagrange point. Thus the discs

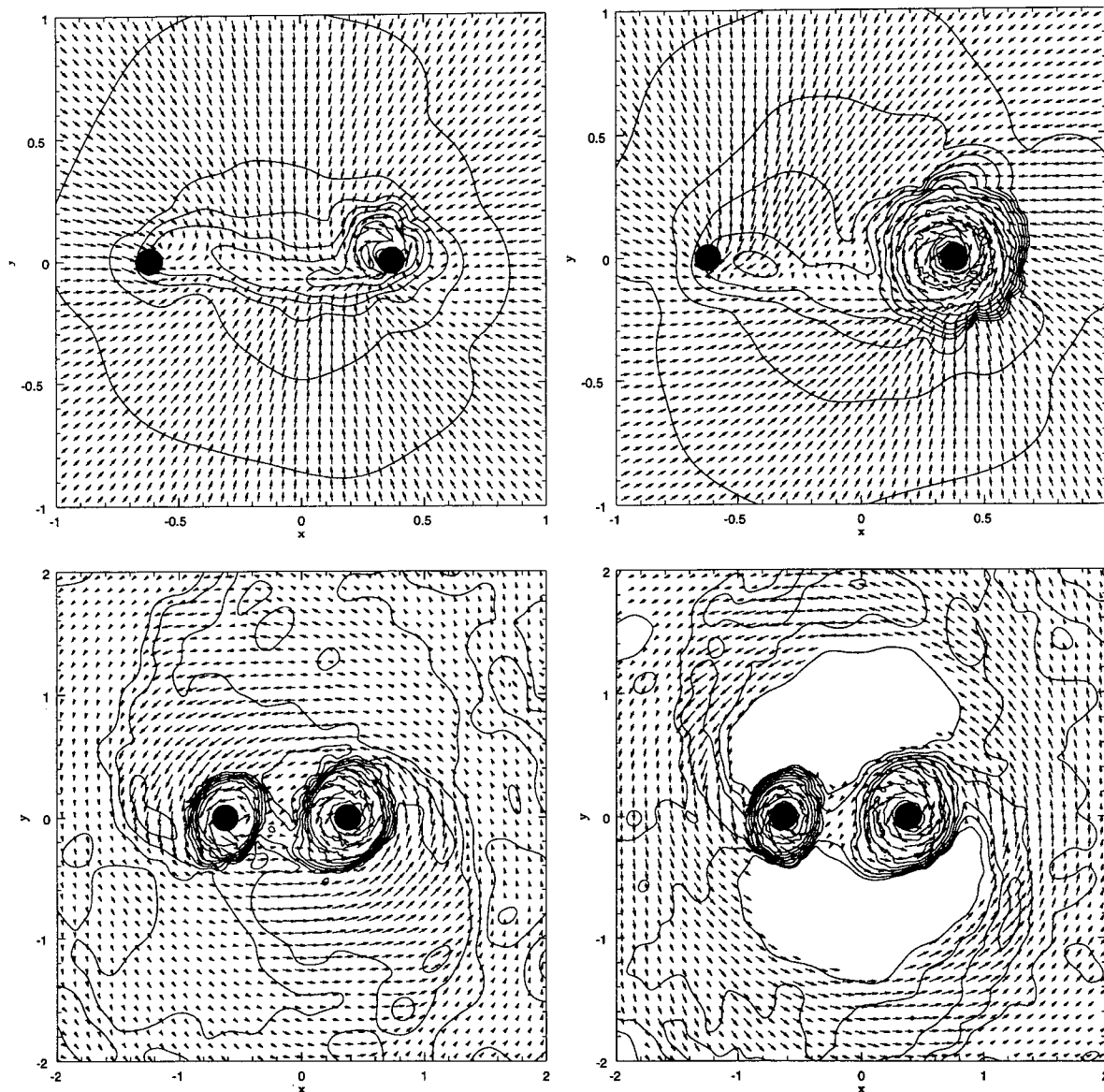


**Figure 3.** Steady-state accretion on to a  $q=0.6$  protobinary system from clouds with specific angular momentum (a)  $j_{\text{inf}}=0.0$  (upper left), (b)  $j_{\text{inf}}=0.4$  (upper right), (c)  $j_{\text{inf}}=0.8$  (lower left) and (d)  $j_{\text{inf}}=1.4$  (lower right). The density and velocity field are given. Density contours are in levels of 0.5 decades, and the length of the arrows is proportional to the speed of the flow in the rest-frame. The protostars are marked with filled circles, with sizes equal to the accretion radii of the sink particles, and with the primary on the right. Axes are given in units of the binary's separation  $D$ .

have large radii and are prone to tidal distortion by the companion. This can cause the discs to overflow the Roche lobes of the protostars, and material to flow between the discs (e.g.,  $j_{\text{inf}}=1.4$ , in Fig. 3). The flow of gas is generally from the circumprimary to the circumsecondary disc, and it therefore increases the relative accretion rate  $\dot{M}_2/\dot{M}_1$ . Finally, note that the infalling gas initially settles into a circumbinary disc at its periastron distance from the centre of mass of the binary, but that it has too much angular momentum to remain there (for a parabolic trajectory, the periastron distance is half the radius of a circular orbit). The material does not form a Keplerian disc at this radius. Rather, the gas spirals outwards to form a Keplerian disc at

the circularization radius. Hence the material that is accreted on to the circumstellar discs, and interacts with the binary via gravitational torques the strongest, is that which is continuously falling on to the system.

With  $j_{\text{inf}}=2.0$ , the circumbinary disc forms a long way from the binary and its inner edge is not perturbed strongly enough by the binary for material to pass inside the outer Lagrange points to form accretion streams on to the circumstellar discs.

Comparing these calculations with previous work, the  $j_{\text{inf}}=0$  gaseous simulations agree qualitatively with the simulations of Monks & Rayburn (1978). They studied the accretion of gas with zero angular momentum on to binaries with

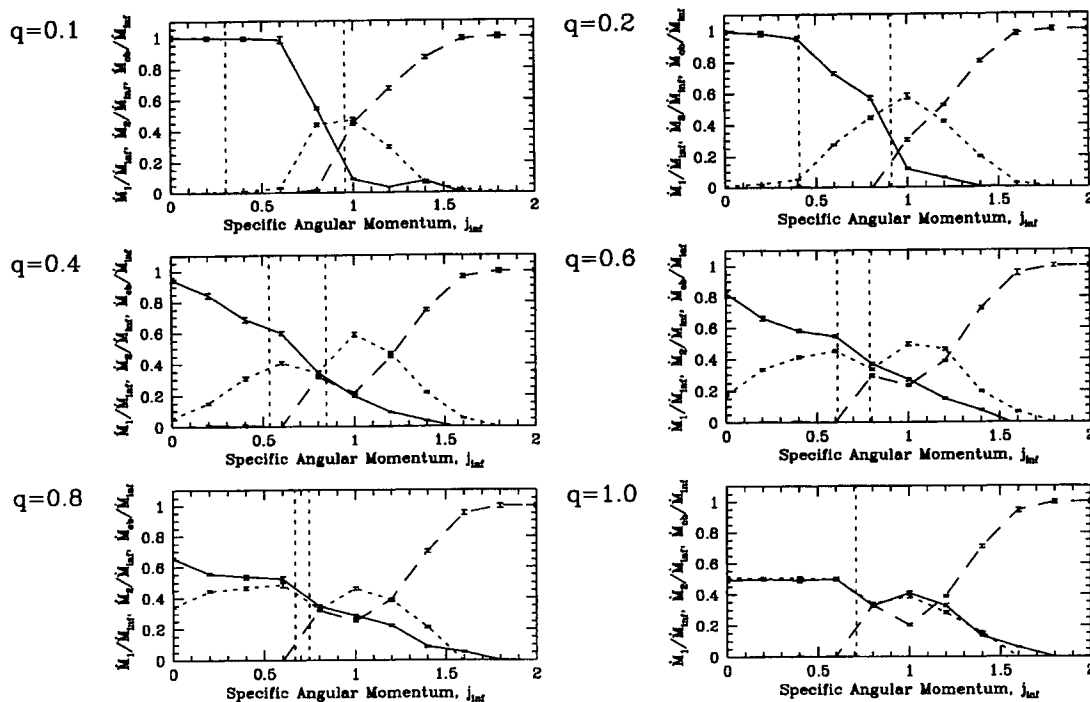


**Figure 4.** The fraction of the infalling cloud material that is accreted by the primary or its circumstellar disc  $\dot{M}_1/\dot{M}_{\text{inf}}$  (solid), the secondary or its circumstellar disc  $\dot{M}_2/\dot{M}_{\text{inf}}$  (dotted), and the circumbinary disc  $\dot{M}_{\text{cb}}/\dot{M}_{\text{inf}}$  (dashed). The fractions are given as functions of the specific angular momentum of the cloud  $j_{\text{inf}}$  for various mass ratios  $q$ . Estimated error bars are given. The vertical lines give the specific angular momentum required for the gas to form a circular orbit at the radius of the primary (left) or secondary (right).

mass ratios of  $q=0.5$  and  $0.25$  with a two-dimensional hydrodynamics code, and found that accretion proceeds via Bondi–Hoyle-type accretion streams on to the inside-trailing edges of the ‘stars’ (modelled by sink cells), as we find here. The radii of their sink cells were  $1/6$  of the binary’s separation, and hence they did not have enough resolution to determine if circumstellar discs were formed by the accretion.

#### 4.2 Circumstellar and circumbinary disc properties

The fractions of the infalling material that are captured by each of the protostars (either via accretion or the formation of circumstellar discs) and the fraction which forms a circumbinary disc are given in Fig. 4 as functions of the binary’s mass ratio and the cloud’s specific angular momentum.

For accretion with low angular momentum, most of the infalling material is captured by the primary, forming a circumprimary disc or being accreted via a Bondi–Hoyle-type accretion stream. For gas with intermediate angular momentum, the fraction captured by the primary decreases, and the fraction captured by the secondary increases. With  $j_{\text{inf}} \approx 0.6\text{--}0.8$  (depending on  $q$ ) a circumbinary disc begins to form; not all of the infalling material is accreted by the protostars and/or their circumstellar discs. For higher  $j_{\text{inf}}$ , an ever-decreasing fraction of the infalling material reaches the circumstellar discs, and finally all the gas goes into a circumbinary disc. The circumbinary disc forms with lower

$j_{\text{inf}}$  infall for higher mass ratios. This is because the secondary is closer to the centre of mass of the binary, and therefore the infalling material does not require as much specific angular momentum to form a disc outside its orbit. Thus circumbinary disc formation begins when  $j_{\text{inf}}$  is slightly less than that required to form a circular orbit at the radius of the secondary (Fig. 4).

From the steady-state accretion flows (Figs 1 and 2), we have seen that the capture of gas by a protostar can occur either via a Bondi–Hoyle-type accretion flow, or the formation of a circumstellar disc. Also, a general progression of larger radii circumstellar discs for infall with higher angular momentum is seen. The presence and size of the circumstellar discs can be quantified by determining the mean specific spin angular momentum of the material that is captured by the protostars ( $s_1$  and  $s_2$  for the primary and secondary, respectively). The gas is either accreted directly or forms circumstellar discs, depending on how much specific angular momentum it has with respect to the protostar. The spins,  $s_1$  and  $s_2$ , are given in Fig. 5 as functions of the mass ratio and  $j_{\text{inf}}$ . For comparison, the spins accreted by the protostars in the ballistic calculations of Paper I are also given (see Section 8). Three distinct regimes are apparent. For low  $j_{\text{inf}}$ , the protostars capture gas that essentially has *no* spin, and therefore circumstellar discs cannot be formed. Rather, the gas forms Bondi–Hoyle-type accretion streams. This is especially true of the secondary (e.g. the  $q=0.6$  binary with  $j_{\text{inf}} \lesssim 0.4$  in Fig. 5). When  $j_{\text{inf}}$  passes some critical value, however, the captured material does carry spin angu-



lar momentum, and circumstellar discs form. The magnitude of the specific spin angular momentum increases roughly linearly with increasing  $j_{\text{inf}}$  above the critical value (e.g. the  $q=0.6$  binary with  $0.4 \lesssim j_{\text{inf}} \lesssim 0.8$  in Fig. 5). Finally, for accretion with high specific angular momentum,  $s_1$  and  $s_2$  saturate at finite values (e.g. the  $q=0.6$  binary with  $j_{\text{inf}} \gtrsim 0.8$  in Fig. 5).

For disc formation, the infalling material must have  $j_{\text{inf}}$  greater than the specific orbital angular momentum of the protostar that captures it so that its excess angular momentum provides spin angular momentum about the protostar (cf. Fig. 5). Thus the criterion for disc formation is that

$$j_{\text{inf}} \gtrsim j_* \text{ where } j_* = \begin{cases} j_1 & \text{for the primary} \\ j_2 & \text{for the secondary,} \end{cases} \quad (5)$$

and the specific orbital angular momenta of the primary and secondary are given by

$$j_1 = \sqrt{GM_b a} \frac{q^2}{(1+q)^2} \quad (6)$$

and

$$j_2 = \sqrt{GM_b a} \frac{1}{(1+q)^2}, \quad (7)$$

respectively. When material is captured by a protostar it obtains the same specific orbital angular momentum as the

protostar, by definition. Therefore, if  $j_{\text{inf}} \lesssim j_*$ , no disc is formed as the gas must obtain the additional angular momentum it needs from the protostar it is captured by. This angular momentum is gained as it falls on to the protostar in the Bondi–Hoyle-type accretion stream. Note that the formation of very small discs may be possible in this case, but higher resolution calculations are required to determine whether this happens or not. If  $j_{\text{inf}} \gtrsim j_*$ , the material does not need any additional specific angular momentum to be captured. Rather, it must lose specific orbital angular momentum; its excess angular momentum goes into spin angular momentum and forces the gas to form a disc around the protostar. This also explains the roughly linear increase of  $s_1$  and  $s_2$  with  $j_{\text{inf}}$  once  $j_{\text{inf}} \gtrsim j_*$ , since more of  $j_{\text{inf}}$  must go into spin angular momentum. Also, because  $j_1 < j_2$  (with the exception of  $q=1$ ),  $s_1 > s_2$ . Note that equation (5) is only approximate, as the material gains a little angular momentum from the binary as it falls in. The primary forms a resolved disc under infall with zero angular momentum in binaries with mass ratios of  $0.3 \lesssim q \lesssim 0.6$  because of this gain of angular momentum (e.g. Fig. 2). For low mass ratios the primary cannot form a resolved disc, as the gravitational torques of the binary are weak and the gas cannot gain enough angular momentum. For high mass ratios no resolved disc is formed because, although the gravitational torques are strong, the gas must gain a lot of specific angular momentum as the primary has a high specific orbital angular momentum. Finally, in all cases, the specific spin angular momentum of the primary  $s_1$ ,

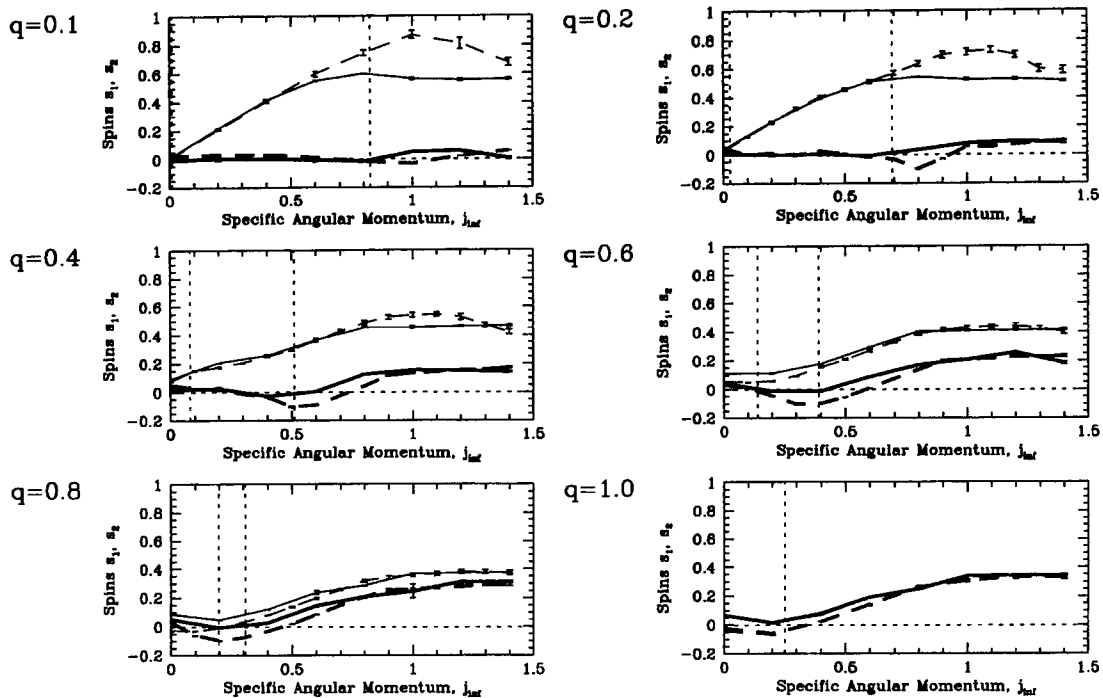


**Figure 5.** The specific spin angular momentum accreted by the primary or its circumstellar disc  $s_1$  (thin lines) and the secondary or its circumstellar disc  $s_2$  (thick lines) in binaries with mass ratios  $q$  which accrete gas with specific angular momentum  $j_{\text{inf}}$ . Results are given for gaseous accretion (solid) and for ballistic accretion from Bate (1996) with accretion radii equal to the mean Roche lobe sizes of the protostars (dashed). Estimated error bars are given. The vertical lines give the specific orbital angular momenta of the primary  $j_1$  (left) and secondary  $j_2$  (right).

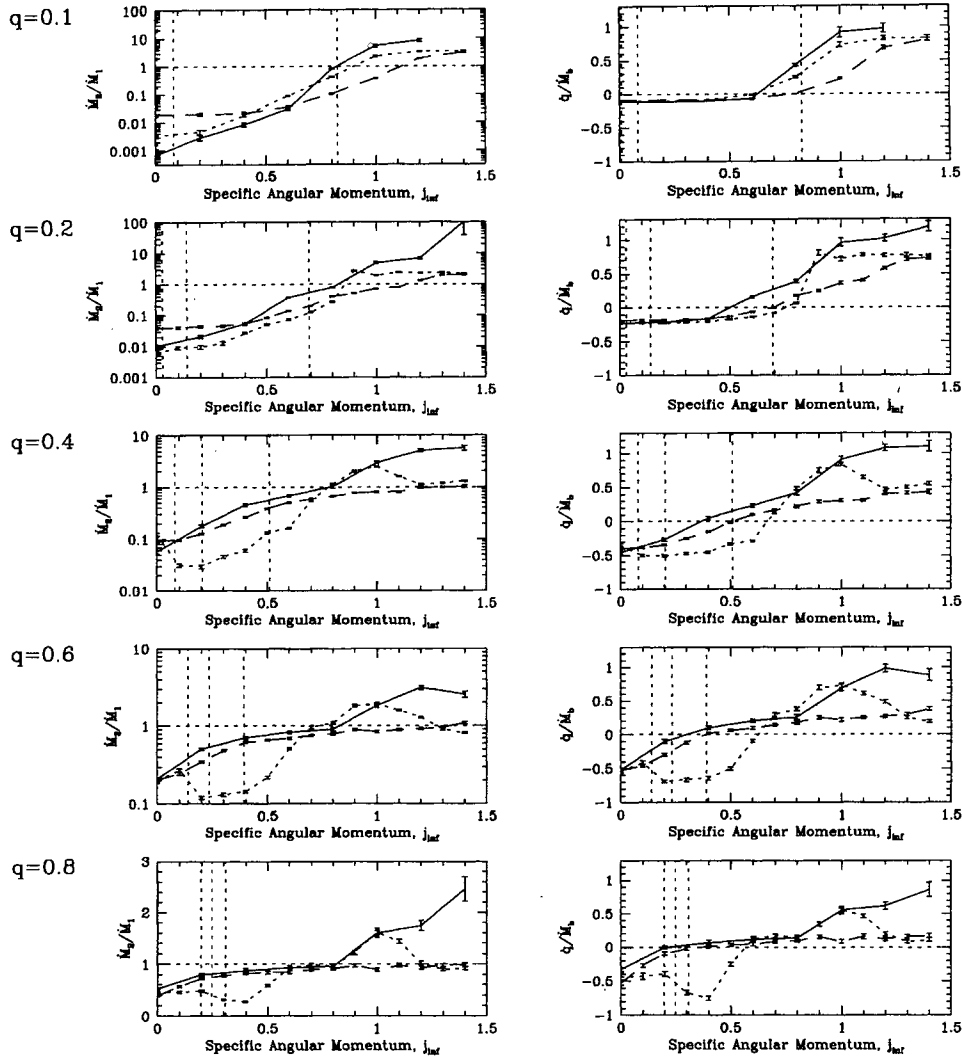


**Figure 6.** The (a) relative accretion rates  $\dot{M}_2/\dot{M}_1$  (left), and (b) rates of change of mass ratio per unit mass accreted  $\dot{q}/\dot{M}_b$  (right), for binaries accreting gas with specific angular momentum  $j_{\text{inf}}$ . Results are given for gaseous accretion (solid) and for ballistic accretion from Bate (1996) with accretion radii of  $r_{\text{acc}} = 0.05D$  (dotted) and  $r_{\text{acc}}$  equal to the mean Roche lobe sizes of the protostars (dashed). Estimated error bars are given. The vertical lines give the specific orbital angular momenta of the primary  $j_1$  (left), binary  $j_b$  (middle) and secondary  $j_2$  (right).

and the secondary  $s_2$  saturate at finite values for high values of  $j_{\text{inf}}$ . As the mass ratio increases, the saturation value of  $s_1$  decreases and that of  $s_2$  increases, until for  $q = 1$  they are the same. The spins saturate because the sizes of the discs are limited roughly to the sizes of the Roche lobes of the protostars by truncation due to resonances (Artymowicz & Lubow 1994).

## 5 RELATIVE ACCRETION RATE AND RATE OF CHANGE OF MASS RATIO

We now consider the relative accretion rate of the two protostars and the resulting rate of change of mass ratio. Note that, from the definitions of  $\dot{M}_1$  and  $\dot{M}_2$ , we assume that all the material in a protostellar disc is eventually accreted by the protostar it orbits. This occurs on a longer (viscous) time-scale than that which is considered here.

Fig. 6 gives the relative accretion rates  $\dot{M}_2/\dot{M}_1$ , and the rates of change of mass ratio per unit mass accreted  $\dot{q}/\dot{M}_b$ . For comparison, the ballistic results from Paper I are also given (see Section 8). Note that the values for  $j_{\text{inf}} = 1.4$  have larger errors than indicated, because the circumstellar discs are only marginally resolved due to the low accretion rate on to them.

Qualitatively, for infall with low angular momentum, the primary accretes most of the material, while, when the cloud's angular momentum is increased, the secondary accretes more relative to the primary. The results are also most extreme with binaries with low mass ratio. For a  $q = 0.1$  binary, the relative accretion rates vary from  $\approx 10^{-3}$  with  $j_{\text{inf}} = 0$ , to  $\approx 10$  with  $j_{\text{inf}} \gtrsim 1.2$ . For higher mass ratios, the variation decreases, until for a  $q = 1$  binary the two components capture the same amount of gas. The variation of the relative accretion rate with  $j_{\text{inf}}$  is simple to explain. With infall with low angular momentum, the gas essentially falls

into the centre of mass of the binary and, hence, is mainly accreted by the primary (which is closest to the centre of mass in a system with low mass ratio). Only the small amount of gas which passes close to the secondary is accreted in a Bondi–Hoyle-type accretion stream. For infall with higher angular momentum, the gas can only fall in to its periastron distance from the centre of mass of the system (in the absence of gravitational torques). This makes accretion by the secondary easier, as the gas does not need to gain as much angular momentum to be captured by it. When a distinct circumbinary disc is formed, the secondary captures more gas than the primary, even though it has a lower mass, because it is closer to the radius to which the gas falls in and, thus, is able to perturb the gas more strongly. Also, some material that does fall on to the circumstellar disc of the primary has high specific angular momentum and is easily perturbed by the secondary to flow over to its disc, further increasing the relative accretion rate. Finally, note that the relative accretion rate equals unity when  $j_{\text{inf}}=0.7-0.8$  (essentially *independent* of the mass ratio of the binary).

Following the relative accretion rate, the mass ratio is found to decrease under accretion with low angular momentum, and increase under accretion with high angular momentum. One of the most important aspects of the effect of accretion on a protobinary system is determining at what value of  $j_{\text{inf}}$  the rate of change of mass ratio changes sign. This is found to occur when  $j_{\text{inf}}$  is slightly less than the specific orbital angular momentum of the secondary  $j_2$  (Fig. 6b). Thus a binary of mass ratio  $q \gtrsim 0.7$  will always increase its mass ratio if the specific angular momentum of the infalling material is greater than the specific angular momentum of the binary, i.e.,

$$j_{\text{inf}} \gtrsim j_b = \sqrt{GM_b a} \frac{q}{(1+q)^2}. \quad (8)$$

For lower mass ratios,  $j_{\text{inf}}$  must be increasingly larger than  $j_b$  for the mass ratio to increase.

## 6 EFFECTS OF ACCRETION ON THE SEPARATION OF THE BINARY

As well as the role that accretion plays in the formation of discs and its effect on the masses of the components of the binary, accretion alters the separation of the binary. Two separate effects are involved. First, there is the accretion itself, which changes the separation due to the addition of mass and angular momentum and the changing of the mass ratio. Secondly, if a circumbinary disc is formed, the binary may transfer orbital angular momentum to the material in the disc via gravitational torques. This loss of orbital angular momentum reduces the separation of the binary. Thus the rate of change of separation of the binary is given by  $\dot{a} = \dot{a}_{\text{acc}} + \dot{a}_{\text{grav}}$ , where  $\dot{a}_{\text{acc}}$  and  $\dot{a}_{\text{grav}}$  are the rates of change of separation due to accretion and due to gravitational torques from the circumbinary disc, respectively. Note that  $\dot{a}_{\text{grav}}$  depends linearly on the shear viscosity (Lubow & Artymowicz 1996) while  $\dot{a}_{\text{acc}}$  is independent of the viscosity. The viscosity of SPH is known to be large (we estimate the effective viscosity parameter  $\alpha_v \sim 0.1$ ), and thus the values of  $\dot{a}_{\text{grav}}$  presented here are likely to be higher than is physical.

To determine these two separate effects, the equation for the orbital angular momentum of a circular binary about its centre of mass,

$$L_b = \sqrt{GM_b^3 a} \frac{q}{(1+q)^2}, \quad (9)$$

is differentiated with respect to time to give

$$\dot{a} = \frac{2(1+q)^2}{q} \sqrt{\frac{a}{GM_b^3}} \dot{L}_b - \frac{3a}{M_b} \dot{M}_b - \frac{2a(1-q)}{q(1+q)} \dot{q}. \quad (10)$$

The rate of change of orbital angular momentum of the binary is contributed to both by accretion of gas and by the loss of angular momentum from the binary to a circumbinary disc (if one is present), so that  $\dot{L}_b = \dot{L}_{\text{acc}} + \dot{L}_{\text{grav}}$ . The value of  $\dot{L}_{\text{grav}}$  is determined by monitoring the angular momentum of the circumbinary material of mass  $M_{\text{cb}}$ . Then,

$$\dot{L}_{\text{grav}} = -(\dot{L}_{\text{cb}} - j_{\text{inf}} \dot{M}_{\text{cb}}), \quad (11)$$

where  $\dot{L}_{\text{cb}}$  is the rate of change of angular momentum of the circumbinary material, and the last term subtracts off the increase in the total angular momentum of  $M_{\text{cb}}$  simply due to more particles being injected into the calculation. Finally, the rate of change of separation due to the loss of orbital angular momentum to the circumbinary disc is

$$\dot{a}_{\text{grav}} = \frac{2(1+q)^2}{q} \sqrt{\frac{a}{GM_b^3}} \dot{L}_{\text{grav}}, \quad (12)$$

and hence both  $\dot{a}_{\text{acc}}$  and  $\dot{a}_{\text{grav}}$  are obtained.

Fig. 7 gives the rates of change of separation per unit mass accreted  $\dot{a}/\dot{M}_b$  and per unit mass of infall  $\dot{a}/\dot{M}_{\text{inf}}$ , as functions of the mass ratio and  $j_{\text{inf}}$ . For Fig. 7(a), only the rate of change of separation due to accretion  $\dot{a}_{\text{acc}}/\dot{M}_b$  is plotted. Comparisons are given from the ballistic calculations of Paper I (see Section 8). We also graph the values of  $\dot{a}_{\text{acc}}/\dot{M}_b$  that would be obtained if *all* the specific angular momentum  $j_{\text{inf}}$  of the captured material was converted into orbital angular momentum of the binary. We assume that  $\dot{q}=0$ , which is a good approximation for  $q \gtrsim 0.3$  [since then the third term in equation (10) is small, even though  $\dot{q} \neq 0$ ]. From equation (10), this is given by

$$\frac{\dot{a}}{\dot{M}_b} = \frac{2(1+q)^2}{q} \sqrt{\frac{a}{GM_b^3}} j_{\text{inf}} - \frac{3a}{M_b}. \quad (13)$$

This is plotted to demonstrate the effect that the conversion of some of the angular momentum of the gas into spin angular momentum of the circumstellar discs has on the final rate of change of separation. For Fig. 7(b), the total effect of gaseous accretion on the separation  $\dot{a}/\dot{M}_{\text{inf}}$  is given, along with the separate effects due to accretion only  $\dot{a}_{\text{acc}}/\dot{M}_{\text{inf}}$ , and due to the transfer of orbital angular momentum to the circumbinary material  $\dot{a}_{\text{grav}}/\dot{M}_{\text{inf}}$ .

### 6.1 Effects due to accretion

The rate of change of separation (due to accretion only) per unit mass accreted ( $\dot{a}_{\text{acc}}/\dot{M}_b$  in Fig. 7a) increases monotonically with  $j_{\text{inf}}$ . This is expected, since the accretion of

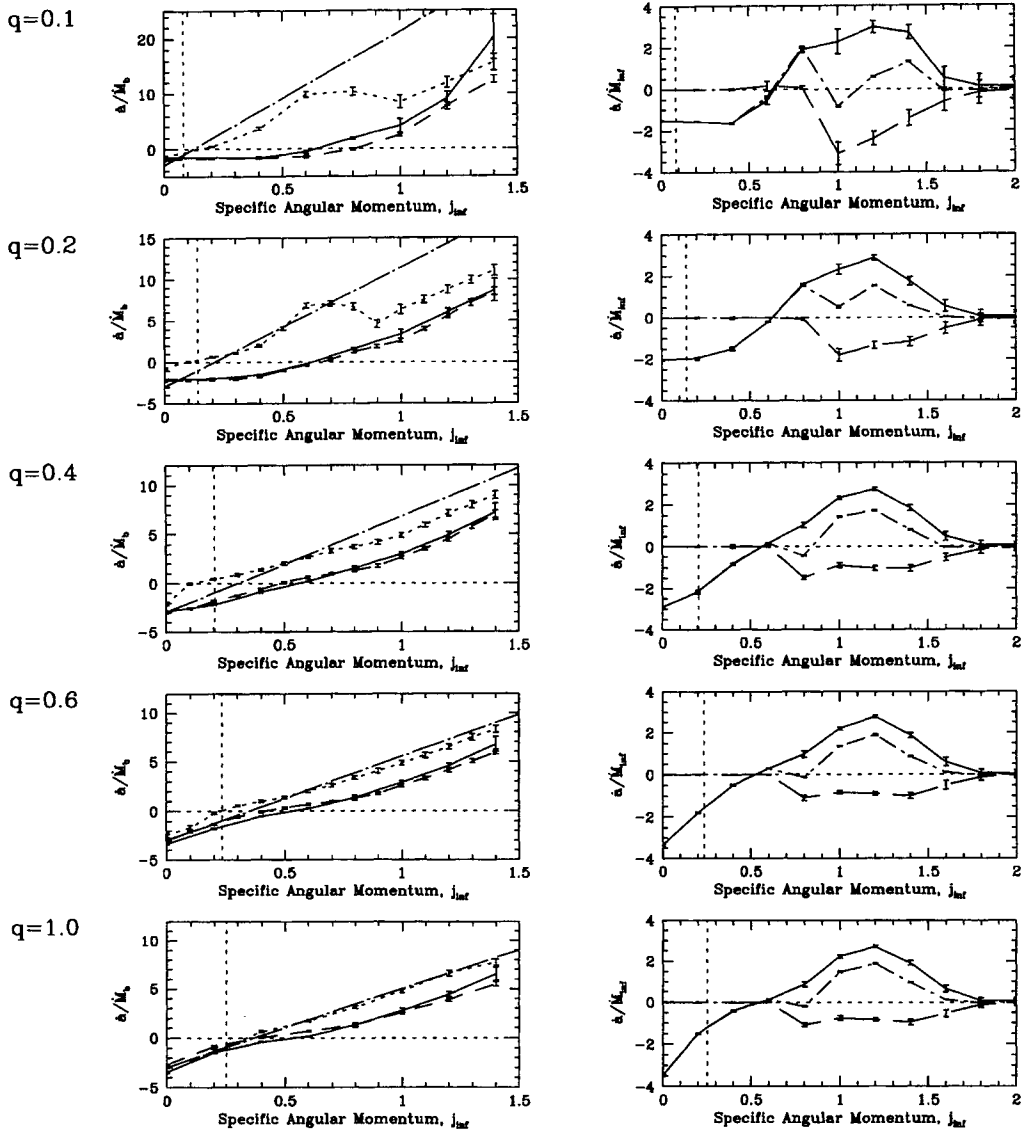


**Figure 7.** The effects on the separations of binaries accreting gas with specific angular momentum  $j_{inf}$ . Graph (a) gives the rate of change of separation due to accretion *only* per unit mass accreted by the binary  $\dot{a}_{acc}/\dot{M}_b$  (left). Results are given for gaseous accretion (solid), and for ballistic accretion from Bate (1996) with accretion radii of  $r_{acc} = 0.05D$  (dotted) and  $r_{acc}$  equal to the mean Roche lobe sizes of the protostars (dashed). Graph (b) gives the rate of change of separation per unit mass of infall for the gaseous calculations (right). With gaseous accretion, the separation is affected both by accretion  $\dot{a}_{acc}/\dot{M}_{inf}$  (solid), and by the loss of orbital angular momentum to the circumbinary disc  $\dot{a}_{grav}/\dot{M}_{inf}$  (long-dashed). The combination of these two effects  $\dot{a}/\dot{M}_{inf}$  is also given (dot-dashed). Estimated error bars are given. The specific orbital angular momentum of the binary  $j_b$  (vertical), and the  $\dot{a}_{acc}/\dot{M}_b$  expected if all the  $j_{inf}$  of the accreted matter was converted to orbital angular momentum (see text), are also given (dot-long-dashed, left).

material with higher specific angular momentum results in a larger increase the specific orbital angular momentum of the binary. Note, however, that the rate of change of separation is nearly always significantly less than if all of the angular momentum of the infalling material was converted to orbital angular momentum of the binary (equation 13). This is because much of the angular momentum goes into the spin angular momentum of the circumstellar discs (see also Section 8).

Considering the rate of change of separation per unit mass of infall  $\dot{a}_{acc}/\dot{M}_{inf}$ , the separation decreases for  $j_{inf} \lesssim 0.6$  almost *independent* of mass ratio (Fig. 7b). Thus, for all mass

ratios, there is a region where the separation decreases, even though  $j_{inf} > j_b$ . For a  $q = 0.1$  binary, the specific angular momentum of the infalling material has to be more than 7 times greater than that of the binary for the separation to increase! For  $j_{inf} \gtrsim 0.6$ , the separation increases, with a peak rate of increase at  $j_{inf} \approx 1.2$ , again independent of the mass ratio. Beyond this the rate of increase of separation decreases, because less material is being accreted by the protostars and their circumstellar discs, and more is forming a circumbinary disc. For  $j_{inf} \gtrsim 1.8$ , there is no accretion on to the circumstellar discs for any mass ratio (Fig. 4) and the binary's separation is constant.

## 6.2 Effects due to circumbinary disc formation

We now consider the effect of the loss of orbital angular momentum to a circumbinary disc. For infall with low angular momentum ( $j_{\text{inf}} \lesssim 0.7\text{--}0.9$ , depending on  $q$ ), gravitational interactions of the binary with the circumbinary material have no effect (Fig. 7b) because there is no build-up of a circumbinary disc (Fig. 4). For infall with high angular momentum, the binary transfers orbital angular momentum into the circumbinary disc and the orbit shrinks ( $\dot{a}_{\text{grav}}/\dot{M}_{\text{inf}}$  in Fig. 7b). The maximum transfer rate generally occurs near the lowest value of  $j_{\text{inf}}$  for which a circumbinary disc forms ( $j_{\text{inf}} \approx 0.8\text{--}1.0$ , depending on  $q$ ). As  $j_{\text{inf}}$  increases, the transfer rate generally decreases again, because the circumbinary disc is not as close to the binary and the gravitational torques rapidly decrease in strength with increasing radius.

## 6.3 Combined effects of accretion on the separation of the binary

When the effects of accretion and interactions with the circumbinary material are combined, the rate of change of separation for  $j_{\text{inf}} \lesssim 0.7\text{--}0.9$  (depending on  $q$ ) is determined purely from accretion. Above this, the gravitational interaction with the circumbinary material gives a lower rate of increase of separation than that purely from accretion. This can even cause the separation to decrease again in the range  $0.8 \lesssim j_{\text{inf}} \lesssim 1.0$ ! However, as noted above, this depends on the shear viscosity. For the highest values of  $j_{\text{inf}}$ , the rate of change of separation goes to zero, because there is no accretion on to the circumstellar discs, and the circumbinary disc is too far from the binary for significant angular momentum to be transferred from the binary to the disc.

## 7 DEPENDENCE OF THE RESULTS ON THE RADIAL-INFALL VELOCITY

We have considered gaseous accretion on to a protobinary system, examining the disc formation process and the effects on the binary's mass ratio and separation. We now briefly consider how these results depend on the radial-infall velocity of gas at the outer boundary of the calculation. The dependence is determined by performing calculations of  $q=0.2$  and  $q=0.6$  binaries with  $v_{\text{rad}}=0$ , rather than with  $v_{\text{rad}}=1$  as in the previous sections.

Qualitatively, the results are independent of the radial-infall velocity. Quantitatively, they differ, but only for  $j_{\text{inf}} \gtrsim 1.0$ . The major difference that decreasing the radial-infall velocity has is that the periastron distance to which the gas falls in is larger. For  $j_{\text{inf}} \lesssim 1.0$ , the effect is negligible because once the gas falls within the orbit of the secondary, dissipation is important and its original radial-infall velocity is forgotten. For  $j_{\text{inf}} \gtrsim 1.0$ , however, the periastron distance determines the radius at which the inner edge of the circumbinary disc is. With  $v_{\text{rad}}=0$  this radius is larger than with  $v_{\text{rad}}=1$ .

This has a negligible effect on the relative accretion rate, the rate of change of mass ratio, the rate of change of separation (due to accretion) per unit mass accreted  $\dot{a}_{\text{acc}}/\dot{M}_{\text{b}}$ , and the specific spin angular momentum of the material in

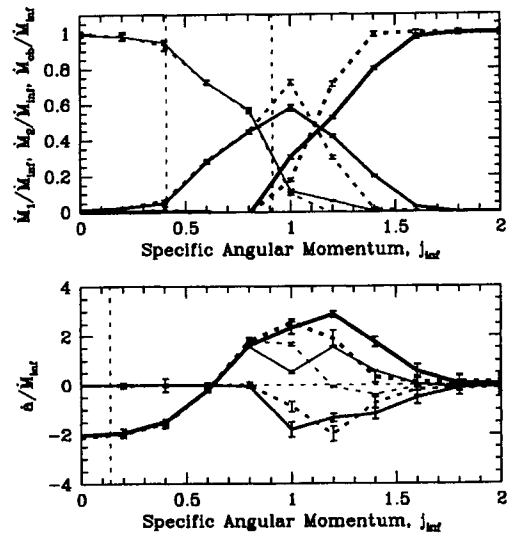


**Figure 8.** The dependence of the results on the radial-infall velocity of the gas at the outer boundary of the cloud. Results are given for a  $q=0.2$  binary as functions of the specific angular momentum of the cloud  $j_{\text{inf}}$  with radial-infall velocities of  $v_{\text{rad}}=1$  (solid) and  $v_{\text{rad}}=0$  (dotted). Plotted are (a) the fractions of the infalling mass accreted by the primary, secondary and circumbinary disc (top), and (b) the rates of change of separation per unit mass of infall (bottom). See Figs 4 and 7 for details.

the circumstellar discs. The main differences that the lower radial-infall velocity has are on quantities directly related to the circumbinary disc. Due to the larger inner radius of the circumbinary disc, less material is captured by the binary and more goes into the circumbinary disc for the same value of  $j_{\text{inf}}$  (Fig. 8a). Thus the rate of change of separation (due to accretion) per unit mass of infall  $\dot{a}_{\text{acc}}/\dot{M}_{\text{inf}}$  is decreased simply because less material is accreted by the circumstellar discs (Fig. 8b). Also, the differences in circumbinary disc formation lead to a different rate of orbital angular momentum loss from the binary to the circumbinary disc (Fig. 8b). For  $j_{\text{inf}} \gtrsim 1.3$ , the effect on the separation due to the gravitational torques is less, because the inner edge of the circumbinary disc is at a larger radius. The overall effect is that a lower radial-infall velocity lowers the rate of change of separation for  $j_{\text{inf}} \gtrsim 1.2$ . The separation is actually found to *decrease* with  $j_{\text{inf}} \gtrsim 1.2\text{--}1.4$  (depending on  $q$ ), because the binary loses more angular momentum to the circumbinary disc than it accretes. This implies that, as the mass of a circumbinary disc becomes large in comparison to the mass that is infalling on to a binary, the separation of the binary may first increase and later decrease, since the effect from material in a Keplerian circumbinary disc is equivalent to reducing the radial-infall velocity at the inner edge of the circumbinary disc to zero. The effects of a Keplerian circumbinary disc on an embedded binary (with no infall on to the system) have been studied by Artymowicz et al. (Artymowicz et al. 1991; Artymowicz & Lubow 1994; Artymowicz & Lubow 1995). As yet, no firm conclusions have been drawn as to whether enough accretion can occur from a Keplerian circumbinary disc to offset the decrease in the binary's separation due to the loss of angular momentum to the circumbinary disc. This requires further study.

## 8 COMPARISON WITH BALLISTIC ACCRETION

We now compare the gaseous accretion results with those obtained in Paper I where the infall was modelled ballistically. Qualitatively, the results are the same. The accretion of gas with low angular momentum lowers the mass ratio and decreases the separation, while accretion with high angular momentum increases the mass ratio and separation. However, with the ballistic calculations, the quantitative results depend on the accretion radii of the protostars which are chosen arbitrarily (Section 1). With gaseous accretion this problem is avoided, because a protostar chooses its own ‘effective accretion radius’. When gas passes inside this radius, it is captured by the protostar due to dissipation of its excess kinetic energy, but the radius at which this occurs is determined purely by the gas dynamics. Gaseous accretion also allows the fraction of the infalling material that forms a circumbinary disc to be determined.

In terms of the rates of change of mass ratio and separation and the specific spin angular momentum of the material captured by a protostar, gaseous accretion is best modelled by ballistic accretion using accretion radii equal to the mean Roche lobe sizes of the protostars, rather than those with small accretion radii of  $r_{\text{acc}} = 0.05D$ . The explanation for this is that, generally, dissipation is not important in determining path of the gas (or its specific angular momentum) as it falls on to the binary. Rather, the role of dissipation is to rid the gas of its excess kinetic energy, if it passes within the Roche lobe of a protostar, so that it can form either a Bondi–Hoyle-type accretion stream or a circumbinary disc. In addition, if the angular momentum of the infalling material is high, dissipation allows a circumbinary disc to form after the gas has fallen on to the plane of the binary. Until this dissipation occurs, the gas essentially falls in ballistically.

The similarity between the gaseous calculations and the ballistic calculations with accretion radii with mean Roche lobe size radii from Paper I is apparent in Fig. 5. This gives the specific spin angular momentum of gas captured by the primary and secondary ( $s_1$  and  $s_2$ ). The agreement is excellent. The only significant difference between the ballistic and gaseous calculations occurs for low mass ratios where the saturation value of  $s_1$  is lower for the gaseous than the ballistic calculations (e.g.,  $q = 0.2$  in Fig. 5). This is probably due to flow of material with high angular momentum from the primary’s to the secondary’s disc (see Section 4.1 and Fig. 1). With ballistic accretion, material, and its angular momentum, cannot be lost once it is accreted by a protostar.

There is also good agreement for the rate of change of separation per unit mass accreted  $\dot{a}_{\text{acc}}/\dot{M}_b$  in Fig. 7(a). This is expected, because the rate of change of separation is primarily determined by the change in orbital angular momentum of the binary and, since the value of the specific spin angular momentum that is captured by the protostars is the same, so is the specific orbital angular momentum that is captured. Note that the ballistic calculations with protostars with small accretion radii give higher rates of change of separation than the gaseous results in almost all cases, because very little spin angular momentum is accreted; nearly all the angular momentum of the gas is converted to

orbital angular momentum when it is accreted, and hence  $\dot{a}/\dot{M}_b$  follows equation (13) very closely (for  $q > 0.5$ ). With gaseous accretion, however, the separation of the binary is no longer affected by accretion alone, but also by the transfer of orbital angular momentum from the binary to the circumbinary disc. Thus, for infall with high specific angular momentum, the overall rate of change of separation is overestimated by the ballistic results.

The relative accretion rates  $\dot{M}_2/\dot{M}_1$  and rates of change of mass ratio per unit mass accreted  $\dot{q}/\dot{M}_b$  for gaseous and ballistic accretion are compared in Fig. 6. For high mass ratios ( $q \gtrsim 0.4$ ) and  $j_{\text{inf}} \lesssim 0.8$ , there is good agreement between the gaseous results and the mean Roche lobe sized ballistic results. The relative accretion rate is higher for gaseous accretion when  $j_{\text{inf}} \gtrsim 0.8$ , mainly due to the formation of a circumbinary disc. The infalling gas settles into a disc, which is perturbed by the components of the binary forming streams of material that flow on to the circumbinary discs. Although the secondary has a lower mass than the primary, it is closer to the inner edge of the disc and thus captures more material. In addition, some material that is captured by the primary is tidally perturbed by the secondary and flows over to its disc, further increasing the relative accretion rate.

## 9 OBSERVATIONAL IMPLICATIONS

Two obvious observational implications arise from the results presented here. First, as noted in Paper I, if a ‘seed’ protobinary forms within a collapsing molecular cloud core and gains a large proportion of its final mass via accretion from the rest of the cloud material, then medium- to long-period binaries are more likely to have low mass ratios, while close binaries are more likely to have equal mass ratios. This is because the specific angular momentum of the infalling material, relative to the binary, is likely to be higher for close binaries than wide binaries. Observations show that low mass ratios are favoured for medium- to long-period binaries (Duquennoy & Mayor 1991); there is weak evidence that equal mass ratios may be favoured for close binaries (Mazeh et al. 1992), although this needs to be confirmed. Note, however, that close binaries could form massive circumbinary discs which may fragment, complicating this picture (Bonnell & Bate 1994a).

The second implication is for the presence of circumbinary discs in pre-main-sequence systems. If a ‘seed’ binary grows to its final mass mainly via the accretion of material with low specific angular momentum, the primary may have a large circumbinary disc, while the secondary is essentially naked. This offers an explanation for the existence of infrared companions to optically visible T Tauri stars. The optically visible star in this scenario would be the secondary, whereas the embedded object would be the primary viewed through its edge-on circumbinary disc. A similar mechanism was proposed by Bonnell & Bastien (1993), who noted that the primary would accrete more material from a collapsing cloud than the secondary, and would thus have a higher extinction. Note that, if there is still infall on to the system, the secondary may even show significant accretion luminosity due to accretion from its own very small circumbinary disc, or even directly from a Bondi–Hoyle-type accretion

stream. The infrared companion systems formed by this method are expected to be fairly wide binaries ( $\approx 100$ -au separation), and there should be no significant circumbinary disc due to the low specific angular momentum of the accreted material. For binaries where a significant circumbinary disc is formed, both stars are expected to form circumstellar discs, although the masses of these discs may differ considerably.

## 10 CONCLUSIONS

In conclusion, we have studied the effects of non-self-gravitating, gaseous accretion on circular protobinary systems. We find that the general behaviour of a binary under accretion is described by a few simple relationships.

First, a circumstellar disc forms around one of the components of the binary only if the specific angular momentum of the infalling gas  $j_{\text{inf}}$  is greater than the specific orbital angular momentum of that component about the centre of mass of the binary. If  $j_{\text{inf}}$  is lower, the protostar accretes via a Bondi–Hoyle-type accretion stream instead. In many cases this results in the primary having a large circumstellar disc, while the secondary has none. If two circumstellar discs are formed, the primary always has a larger radius disc than the secondary and the radii of the circumstellar discs increase with  $j_{\text{inf}}$ , because more of the angular momentum of the captured gas is converted into spin angular momentum of the disc rather than orbital angular momentum. The circumstellar discs have maximum sizes of approximately the Roche lobe radius of the protostars.

Secondly, circumbinary disc formation begins when  $j_{\text{inf}}$  approaches the specific angular momentum required for it to form a circular orbit at the distance of the secondary from the centre of mass of the system.

Thirdly, the mass ratio decreases for the accretion of material with low angular momentum, but starts to increase when  $j_{\text{inf}}$  approaches the specific orbital angular momentum of the secondary  $j_2$ .

Finally, the separation decreases for  $j_{\text{inf}} \lesssim 0.6$  and generally increases above this value, independent of the mass ratio. This means that, for all mass ratios, there is a region where the separation decreases, even though the infalling material has significantly more specific angular momentum than the binary itself ( $j_{\text{inf}} > j_b$ ). When a circumbinary disc is present, the binary loses orbital angular momentum to it via gravitational torques, and this decreases the rate of change of separation over that given purely by the accretion of gas. This effect generally is not strong enough to decrease the separation for  $j_{\text{inf}} \gtrsim 0.6$ , but this conclusion depends on the viscosity and radial-infall velocity of the gas.

## ACKNOWLEDGMENTS

We are grateful to Cathie Clarke and Jim Pringle for many helpful discussions. We thank Cathie Clarke and Melvyn Davies for their critical reading of various versions of the manuscript. We are also grateful to the IoA system managers for their dedication to providing the best possible computing resources. MRB acknowledges scholarships from the Cambridge Commonwealth Trust and the William

Georgetti Memorial Trust, and an ORS award. IAB is grateful to PPARC for financial support.

## REFERENCES

- Adams F. C., Ruden S. P., Shu F. H., 1989, *ApJ*, 347, 959  
 Artymowicz P., Lubow S. H., 1994, *ApJ*, 421, 651  
 Artymowicz P., Lubow S. H., 1995, in Staude H. J., eds, *Disks and Outflows around Young Stars*. Springer-Verlag, Berlin  
 Artymowicz P., Clarke C. J., Lubow S. H., Pringle J. E., 1991, *ApJ*, 370, L35  
 Bate M. R., 1995, PhD thesis, Univ. Cambridge  
 Bate M. R., 1997, *MNRAS*, 285, 16 (Paper I, this issue)  
 Bate M. R., Bonnell I. A., Price N. M., 1995, *MNRAS*, 277, 362  
 Benz W., 1990, in Buchler J.R., ed., *The Numerical Modeling of Nonlinear Stellar Pulsations: Problems and Prospects*. Kluwer, Dordrecht, p. 269  
 Benz W., Bowers R. L., Cameron A. G. W., Press W., 1990, *ApJ*, 348, 647  
 Bonnell I. A., 1994, *MNRAS*, 269, 837  
 Bonnell I., Bastien P., 1992, *ApJ*, 401, 654  
 Bonnell I., Bastien P., 1993, *ApJ*, 406, 616  
 Bonnell I. A., Bate M. R., 1994a, *MNRAS*, 269, L45  
 Bonnell I. A., Bate M. R., 1994b, *MNRAS*, 271, 999  
 Bonnell I., Martel H., Bastien P., Arcoragi J.-P., Benz W., 1991, *ApJ*, 377, 553  
 Bonnell I., Arcoragi J.-P., Martel H., Bastien P., 1992, *ApJ*, 400, 579  
 Boss A. P., 1986, *ApJS*, 62, 519  
 Boss A. P., Bodenheimer P., 1979, *ApJ*, 234, 289  
 Chelli A., Zinnecker H., Carrasco L., Cruz-Gonzalez I., Perrier C., 1988, *A&A*, 207, 46  
 Duquennoy A., Mayor M., 1991, *A&A*, 248, 485  
 Dutrey A., Guilloteau S., Simon M., 1994, *A&A*, 286, 149  
 Fischer D. A., Marcy G. W., 1992, *ApJ*, 396, 178  
 Frank J., King A. R., Raine D. J., 1985, *Accretion Power in Astrophysics*. Cambridge Univ. Press, Cambridge, p. 56  
 Ghez A. M., Neugebauer G., Matthews K., 1993, *AJ*, 106, 2005  
 Heemskerk H. M., Papaloizou J. C., Savonije G. J., 1992, *A&A*, 260, 161  
 Kopal Z., 1959, *Close Binary Systems (International Astrophysics Series, Vol. 5)*. Chapman & Hall Ltd, London, p. 79  
 Leinert Ch., Weitzel N., Zinnecker H., Christou J., Ridgeway S., Jameson R., Haas M., Lenzen R., 1993, *A&A*, 278, 129  
 Lubow S. H., Artymowicz P., 1996, in Wijers R. A. M. J., ed., *Evolutionary Processes in Binary Stars*. Kluwer, Dordrecht, p. 53  
 Mathieu R. D., 1992a, in McAlister H. A., Hartkopf W. I., eds, *Proc. IAU Colloq. 135, Complementary Approaches to Double and Multiple Star Research*. Astron. Soc. Pac., San Francisco, p. 30  
 Mathieu R. D., 1992b, in Duquennoy A., Mayor M., eds, *Binaries as Tracers of Stellar Formation*. Cambridge Univ. Press, Cambridge, p. 155  
 Mathieu R. D., 1994, *ARA&A*, 32, 465  
 Mathieu R. D., Walter F. M., Myers P. C., 1989, *AJ*, 98, 987  
 Mayor M., Duquennoy A., Halbwachs J.-L., Mermilliod J.-C., 1992, in McAlister H. A., Hartkopf W. I., eds, *Proc. IAU Colloq. 135, Complementary Approaches to Double and Multiple Star Research*. Astron. Soc. Pac., San Francisco, p. 73  
 Mazeh T., Goldberg D., Duquennoy A., Mayor M., 1992, *ApJ*, 401, 265  
 Monaghan J. J., 1992, *ARA&A*, 30, 543  
 Monaghan J. J., Gingold R. A., 1983, *J. Comput. Phys.*, 52, 374  
 Monks A. W., Rayburn D. R., 1978, *PASP*, 90, 574  
 Nelson R., Papaloizou J. C., 1993, *MNRAS*, 265, 905  
 Reipurth B., Zinnecker H., 1993, *A&A*, 278, 81

48 *M. R. Bate and I. A. Bonnell*

- Shu F. C., Tremaine S., Adams F. H., Ruden S. P., 1990, ApJ, 358, 495  
Simon M., Chen W. P., Howell R. R., Slovik D., 1992, ApJ, 384, 212  
Strom K. M., Strom S. E., Edwards S., Cabrit S., Strutskie M. F., 1989, AJ, 97, 1451

- Strutskie M. F., Dutkevich D., Strom S. E., Edwards S., Strom K. M., Shure M. A., 1990, AJ, 99, 1187  
Woodward J. W., Tohline J. E., Hachisu I., 1994, ApJ, 420, 247  
Zinnecker H., Wilking B. A., 1992, in Duquennoy A., Mayor M., eds, Binaries as Tracers of Stellar Formation. Cambridge Univ. Press, Cambridge, p. 526